AIAA JOURNAL
Vol. 49, No. 11, November 2011

# Technical Notes

## Analysis of Interacting, Underexpanded, Rarefied Jets

Wenhai Li* and Foluso Ladeinde†
*Stony Brook University, Stony Brook, New York 11794-2300*

DOI: 10.2514/1.J050860



### Nomenclature

| | | |
|---|---|---|
| $D$ | = | diameter of orifice, m |
| $d$ | = | diameter of gas molecule, m |
| $D_M$ | = | diameter of Mach disk |
| $Kn$ | = | Knudsen number |
| $L$ | = | separation distance of orifices, m |
| $P$ | = | pressure, Pa |
| $Re$ | = | Reynolds number |
| $T$ | = | temperature, K |
| $X_M$ | = | location of Mach disk |
| $Z_r$ | = | rotational collision number |
| $\gamma$ | = | specific heat ratio |
| $\lambda$ | = | mean free path, m |

*Subscripts*

| | | |
|---|---|---|
| $b$ | = | background gas |
| $p$ | = | penetration |
| $r$ | = | rotational mode |
| $s$ | = | stagnation conditions |
| $t$ | = | translational mode |

### I. Introduction

THE interaction between rarefied free jets expanding into vacuum has received some attention in recent years because of the relevance to rockets and other space vehicles [1–3]. Rapidly expanding plumes at high altitudes involve the entire range of flow regimes, from continuum flows near the nozzle exit to transitional and free molecular flows at large distances from the nozzle. Furthermore, for flight at different altitudes, the plumes from the spacecraft exhaust may be expanded into a background with finite pressure for the flight in the Earth's atmosphere, or into vacuum, for flight in outer space. Therefore, rarefaction effects are expected to play significant roles. Experimental investigations are expensive and encounter practical difficulties, making numerical analysis an attractive option [4]. This Note focuses on the simulation of the interaction of rarefied jets in the presence of background pressure. We are not aware of a previous simulation exercise for this case. It is pointed out that a numerical investigation of the problem is extremely challenging, even for the direct simulation Monte Carlo (DSMC) approach, and the present work represents the first such simulation. Among other things, the simulation in this Note is made possible by the adaption of the particle conservation method [5] for the implementation of the pressure boundary conditions in DSMC.

### II. Numerical Method and Its Validation

A parallel three-dimensional DSMC program was developed for the present study, using procedures similar to those by Bird [6]. In the current implementation, the variable soft sphere molecular model is used, with Bird's no time counter algorithm for the collision mechanics. The Borgnakke–Larsen phenomenological model is used for the rotational-translational relaxation process, and the time step size is chosen to be smaller than the molecular mean collision interval at the jet stagnation conditions. Automatic, adaptive domain decomposition is used to obtain load balancing in the parallel simulation of the problem. It is pointed out that the number of particles, not the physical size of the domain, determines the computational loads, and hence the load balancing. As has been mentioned above, the implementation of the downstream boundary conditions follows the particle conservation procedure in Wu et al. [5]. To reduce any statistical error from this method, the calculated mean flow velocities in the boundary cells are averaged over time.

To validate the developed code, a single sonic underexpanded nitrogen jet, issuing into a three-dimensional rectangular chamber at specified levels of the background pressure and density, was studied. The stagnation pressure ($P_s$) and temperature ($T_s$) of the jet were 30 torr and 293 K, respectively. Several values of stagnation-to-background pressure ratios ($P_s/P_b$) between 10 and values that approach infinity are investigated, while the background temperature ($T_b$) is set to the source stagnation temperature. Three values of the stagnation Knudsen number ($Kn_s$), 0.05, 0.005, and 0.002, are computed for each $P_s/P_b$ value. More than 27 million particles and 5 million grid cells are used for small Knudsen number calculations ($Kn_s = 0.002$), and approximately 12 million particles and 1.2 million cells for $Kn_s = 0.02$ case. The computational domain is rectangular with size $30D \times 7D \times 7D$ (Fig. 1). The jet flow exhausts through a circular orifice located at the $x = 0$ plane. Only a quarter of the full physical domain is simulated on the assumption of symmetry, with symmetry conditions imposed on both the $y = 0$ and $z = 0$ planes. For the $x = 0$ plane, sonic conditions are used for the particles entering through the orifice and the orifice plate is assumed to be a fully diffusive wall with a temperature value that is equal to the background temperature. The background pressure $P_b$ and temperature $T_b$ are specified for all outflow boundaries.

For jets expanding into vacuum ($P_s/P_b \to \infty$) from a sonic orifice, the only flow parameter is the jet stagnation Knudsen number $Kn_s$, which is also related to the Reynolds number at the orifice exit $Re_D^*$:

$$Kn_s = \frac{\lambda_s}{D} = \frac{k}{\sqrt{2}\pi d^2} \cdot \frac{T_s}{P_s D} = \frac{1}{Re_D^*} \sqrt{\frac{\pi\gamma}{2}} \cdot \left(\frac{2}{\gamma+1}\right)^{1/(\gamma-1)} \tag{1}$$

Therefore, for a fixed temperature $T_s$, $Kn_s$ ($Re_D^*$) is determined only by the product of $P_s$ and $D$. Marrone [7] and Mori et al. [8] experimentally measured the centerline properties of free jets for the case where $P_s D = 15$ torr · mm ($Kn_s = 2.736 \times 10^{-3}$). In Fig. 2, the density distribution along the jet centerline that is calculated with the DSMC code is compared with the experimental data, an asymptotic relation [3], the isentropic relation [9], and the result from a Navier–Stokes simulation (using AEROFLO [10]). Two DSMC calculations are shown: 1) $P_s = 3$ torr, $D = 5$ mm; and 2) $P_s =$ 30 torr, $D = 0.5$ mm. These two calculations give essentially the same results because the product $P_s D$ is the same. Also, the

Presented as Paper 2010-6967 at the 46th AIAA/ASME/SAE/ASEE Joint Propulsion Conference, Nashville, TN, 25–28 July 2010; received 1 September 2010; revision received 23 May 2011; accepted for publication 8 June 2011. 

*Graduate Research Assistant, Department of Mechanical Engineering.
†Department of Mechanical Engineering, Life Member and Associate Fellow AIAA.

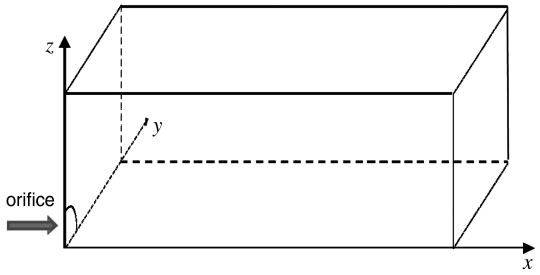


**Fig. 1 Computational domain for the DSMC calculation of underexpanded jets, showing a quarter of the full domain.**

Navier–Stokes simulations, as well as the asymptotic distribution and the isentropic relation, give similar density profiles. The experimental data also agree with these results for $X/D \lesssim 12$, with deviations further downstream. We believe the deviations are due to the inability to obtain perfect vacuum conditions in the experiment, whereas the various calculations have no difficulties enforcing an essentially infinite value for $P_s/P_b$. In Fig. 3, the DSMC results for the rotational temperature distribution along the jet centerline are compared with the experimental data from Marrone [7] and Mori et al. [8]. In this plot, an approximate relation

$$T_r = 0.378 \times T_s \times (X/D)^{-0.8} + 7.096 \times (X/D)^{0.408} \times Z_r \quad (2)$$

developed in a previous work by Li [11], is also shown. The DSMC calculations and the distribution from Eq. (2) are based on $Z_r = 2$. Good agreement with the experimental results is evident.

For jets expanding into a background with finite pressure and the flow in the near-continuum regime, a shock-cell structure is formed due to the strong interaction between the jet flow and background gas. In this case, a rarefaction parameter $\xi$ [12] can be written as

$$\xi \equiv D(P_s \cdot P_b)^{1/2}/T_s = \frac{k}{\sqrt{2}\pi d^2} \cdot \frac{1}{(P_s/P_b)^{1/2} Kn_s} = \frac{k}{\sqrt{2}\pi d^2} \cdot \sqrt{\frac{2}{\pi\gamma}} \cdot \left(\frac{\gamma+1}{2}\right)^{1/(\gamma-1)} \cdot \frac{Re_D^*}{(P_s/P_b)^{1/2}} \quad (3)$$

Thus, rarefaction effects for jets expanding into a background with finite pressure depend on two parameters: $Kn_s$ and $P_s/P_b$. Figure 4 shows a comparison of the current calculations with the experimental data of Ashkenas and Sherman [13] and Crist et al. [14], with good agreement. The foregoing validates the pressure boundary conditions used in this work.

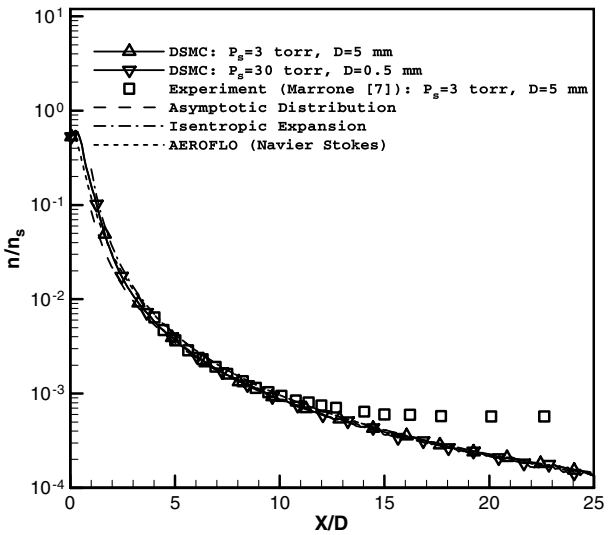


**Fig. 2 Density distributions along the jet centerline for expansion into vacuum ($P_sD = 15$ torr · mm. Two DSMC results with different flow conditions are shown.**

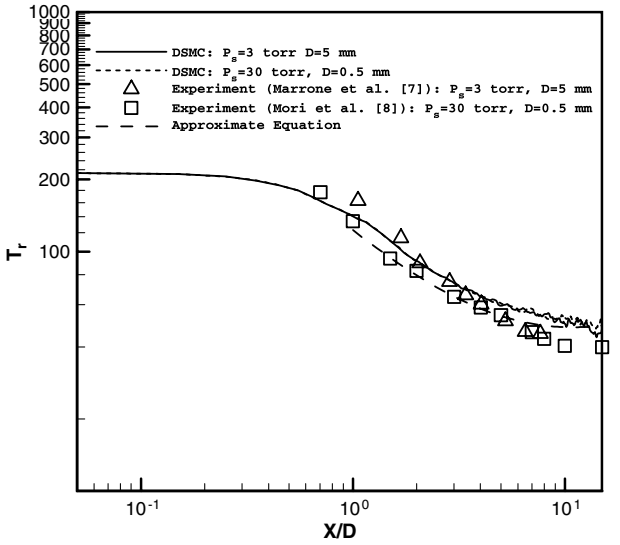


**Fig. 3 Comparison of calculated rotational temperature distribution along the centerline with Marrone [7] and Mori et al.'s [8] experimental data, and the derived rotational temperature decay model [Eq. (2)]. Note that both DSMC and Eq. (2) are calculated for $Z_r = 2$.**

## III. Investigation of Interacting Jets

The physics of dual, interacting jets were investigated. The computational domain is similar to that for the single jet, except that the orifice is now located at $(0, 0, L/2)$. The values of the stagnation Knudsen number $Kn_s$ chosen for the study are 0.02, 0.005, and 0.002, and the separation between the orifices is within $1.0 \leq L/D \leq 8.0$. The values of the stagnation-to-background pressure ratio $P_s/P_b$ are 50, 100, 200, and values that approach infinity. The stagnation pressure and temperature of the jet flow are $P_s = 870$ Pa and $T_s = 285$ K, respectively.

### A. Expansion into Vacuum

The interaction between the two jets can be described in terms of the penetration Knudsen number [3]:

$$Kn_p \equiv \frac{\lambda_p}{l_{\text{ref}}} = \frac{2\sqrt{2}}{\sqrt{\pi}} \sqrt{1+\frac{1}{\gamma}} \cdot \frac{Kn_s}{A} \cdot \frac{L}{D} \cdot \frac{1}{f(\theta)\sin^2\theta} = \frac{2\sqrt{2}}{\sqrt{\pi}} \sqrt{1+\frac{1}{\gamma}} \cdot \frac{Kn_s}{A} \cdot \frac{L}{D} \cdot g(\theta) \quad (4)$$

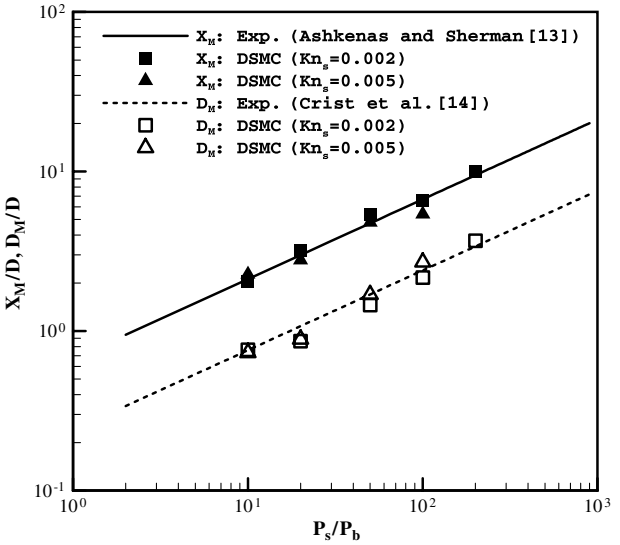


**Fig. 4 Location and diameter of the Mach disk as a function of pressure ratio, showing agreement between experimental data [13,14] and the present DSMC calculations.**

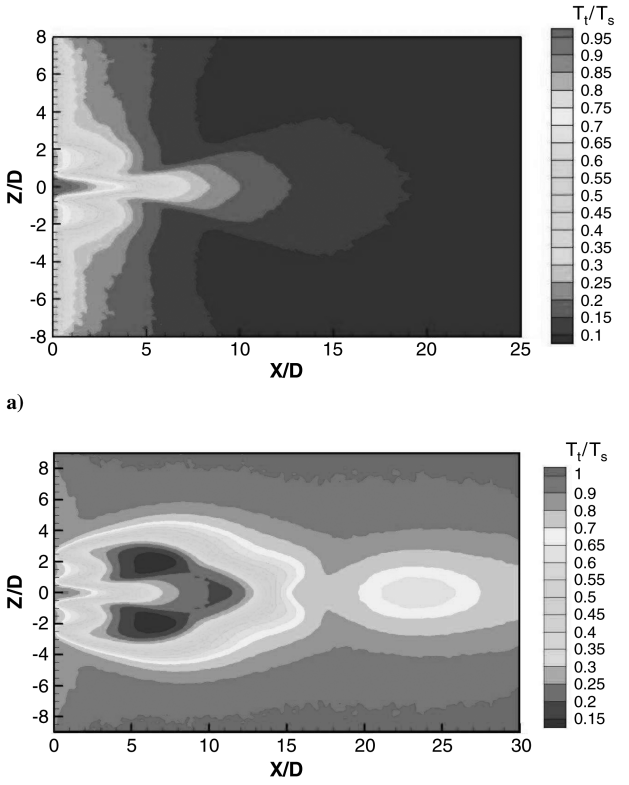


**Fig. 5 Nondimensional translational temperature contours for $Kn_s = 0.002$, $L/D = 3$ when a) jets expand into vacuum, and b) jets expand into a background with $P_s/P_b = 220$.**

where $\lambda_p$ is the penetration mean free path; $l_{\text{ref}}$ represents the characteristic length of the flow, which is chosen as the distance from the symmetry plane to the centerline of the plume; $L/D$ is the orifice separation distance; $g(\theta)$ is a function of the interaction angle $\theta$; and

$$g(\theta) = \left[\cos^2\left(\frac{\pi}{2}\cdot\frac{\theta}{\theta_{\max}}\right)\sin^2\theta\right]^{-1} \tag{5}$$

where $A = 0.345$ and $\theta_{\max} = 95.2°$ for $\gamma = 1.4$. The interaction between the two jets can also be characterized by $Kn_{p,\min}$, which is

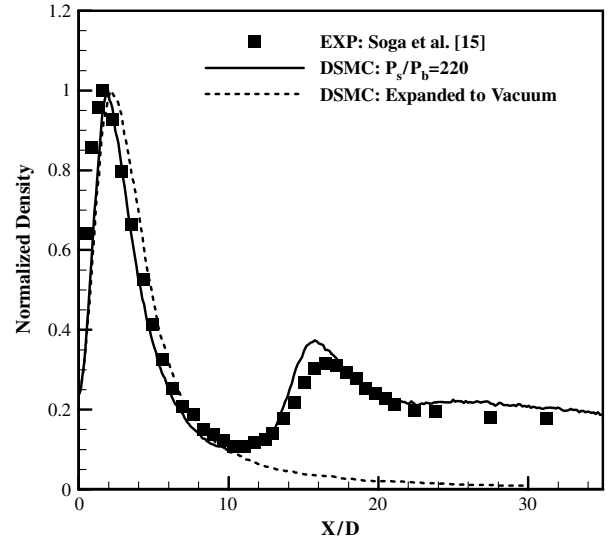


**Fig. 6 Density distribution along the $(x, 0, 0)$ axis showing the comparison with Soga et al.'s experimental data [15] for the case $L/D = 3.0$, $P_s/P_b = 220$, and $Kn_s = 0.002$. Case $P_s/P_b \to \infty$ is shown as a reference.**

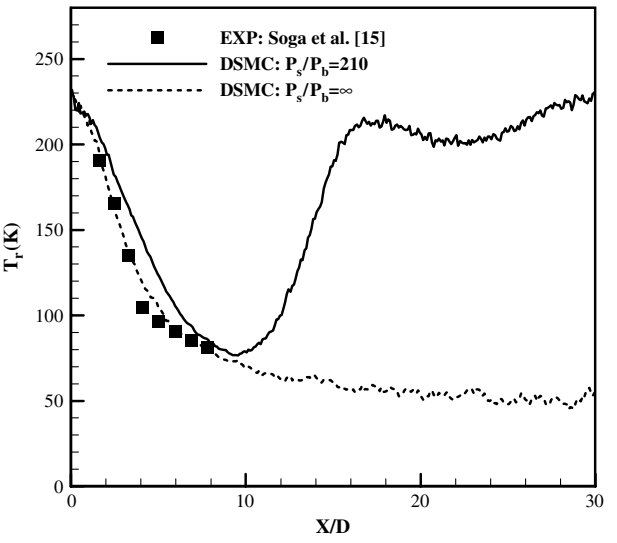


**Fig. 7 Rotational temperature distribution along the $(x, 0, 0)$ axis showing comparison with Soga et al.'s experimental data [15] for the cases $L/D = 3.0$, $P_s/P_b = 210$, and $Kn_s = 0.0027$. Case $P_s/P_b \to \infty$ is shown as a reference.**

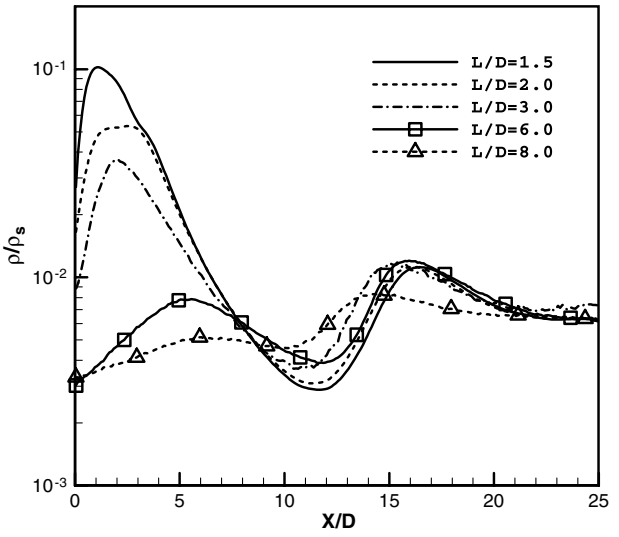


**Fig. 8 Calculated density distributions along the $(x, 0, 0)$ symmetry axis for $Kn_s = 0.002$, $P_s/P_b = 220$, with $L/D = 1.5$, 2.0, 4.0, 6.0, and 8.0.**

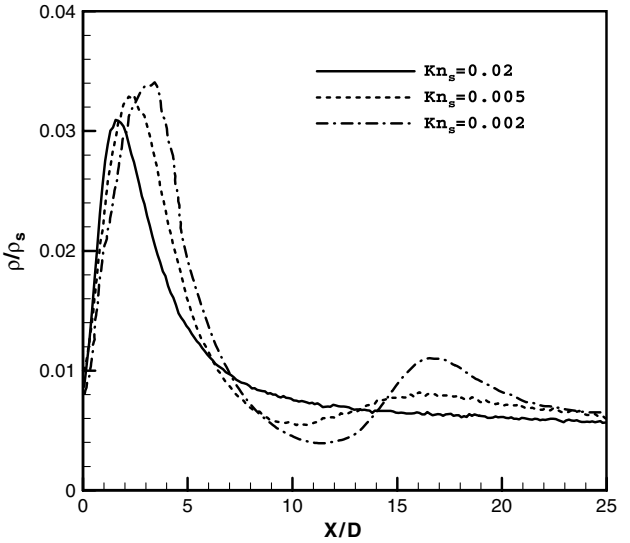


**Fig. 9 Calculated density distributions along the $(x, 0, 0)$ symmetry axis for $P_s/P_b = 200$, $L/D = 3.0$, with $Kn_s = 0.02$, 0.005, and 0.002.**

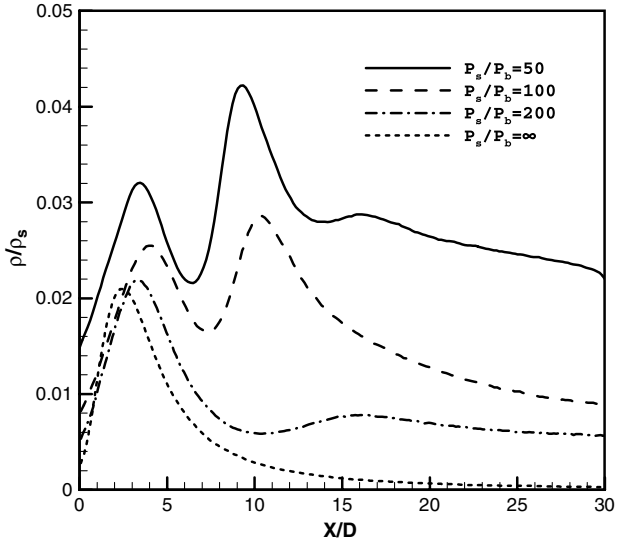


**Fig. 10 Calculated density distributions along the $(x, 0, 0)$ symmetry axis for $Kn_s = 0.005$, $L/D = 3.0$, with $P_s/P_b = 50$, 100, 200, and $\infty$.**

the value of $Kn_p$ when $g(\theta)$ attains its minimum value, which occurs when $\theta \approx 39°$.

### B. Expansion into a Region with Finite Pressure

In this case, the interaction between the molecules of the gases in the two jets and that between the jet gas molecules and the background gas molecules need to be considered. The three parameters, $Kn_s$, $L/D$, and $P_s/P_b$, characterize the overall rarefaction effects.

Soga et al. [15] experimentally measured the density and rotational temperature in interacting jets when $Kn_s = 0.002$ and $P_s/P_b = 220$ for several values of $L/D$. This provides additional validation data for the present effort. The details of the conditions can be found in [15].

Figure 5b shows the translational temperature at the $y = 0$ symmetry plane for $L/D = 3$, $Kn_s = 0.002$, and $P_s/P_b = 220$. Compared with the results of the jets expanding into vacuum (Fig. 5a), it can be seen that the existence of the background pressure significantly changes the flow structure. Although the flow is sill rarefied and the shock structure is much diffused, the primary and secondary shock-cell structures can still be observed. Note that the interaction region between the two primary jets is generally referred to as the secondary jet.

The calculated results are compared with Soga et al.'s experimental data in Fig. 6, which shows the density distribution along the $(x, 0, 0)$ symmetry axis [15]. Note that two sets of DSMC results are presented: $P_s/P_b = 220$ and $P_s/P_b \to \infty$. The monotonic decay of density after the first peak for the case $P_s/P_b \to \infty$ appears reasonable. Dagum and Zhu [2] also simulated this problem, but they assumed that the jet expanded into vacuum. It is therefore not surprising that their result only compared well with Soga et al.'s data [15] when $X/D < 10$. Other investigations using a similar background condition (vacuum) in their simulation do not show results for $X/D \geq 10$ in their comparison with Soga's experiments, suggesting inaccurate results in this region. In our simulation, the correct background conditions ($P_s/P_b = 220$) are used and our predictions compare well with experimental data at all $X/D$ values.

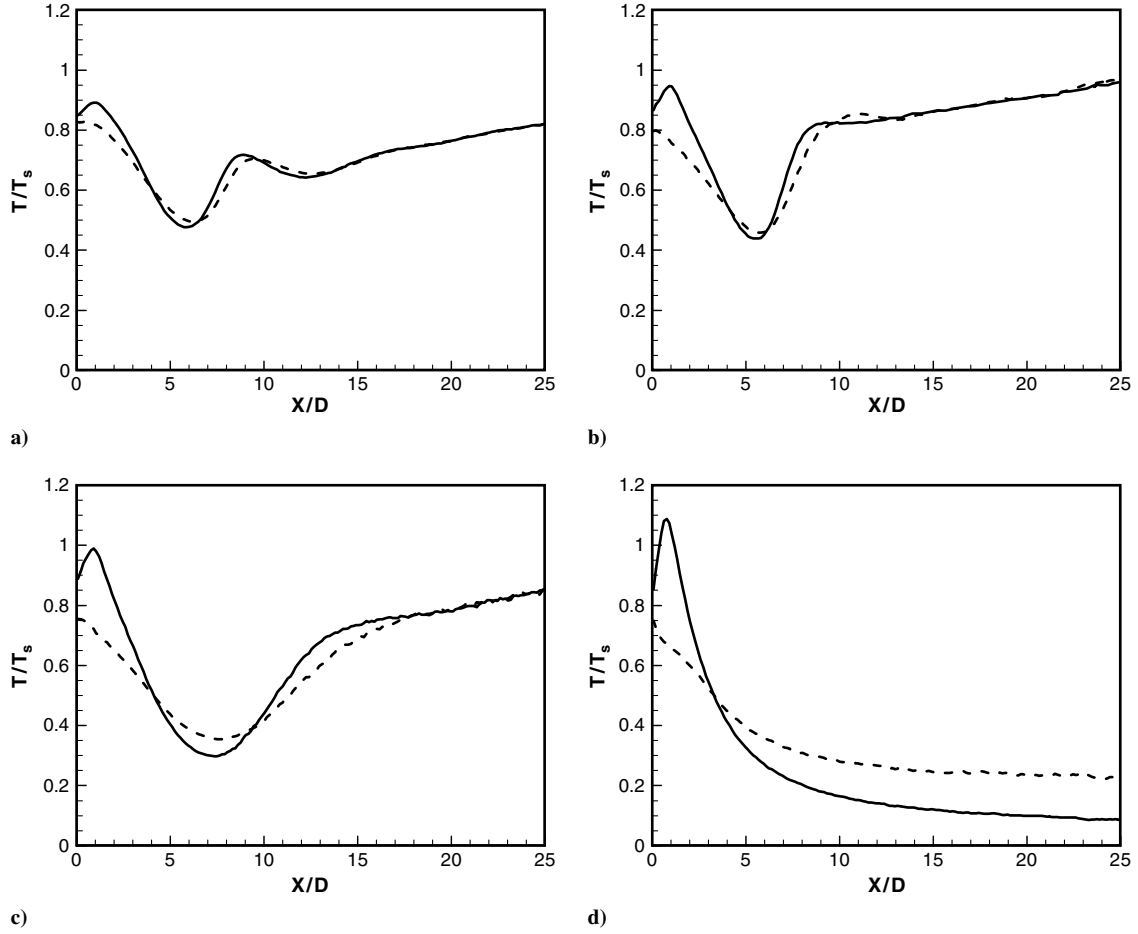


**Fig. 11 Calculated translational temperature (solid lines) and rotational temperature (dashed lines) distributions along the $(x, 0, 0)$ symmetry axis for $Kn_s = 0.005$, $L/D = 3.0$, with different values of $P_s/P_b$: a) $P_s/P_b = 50$; b) $P_s/P_b = 100$; c) $P_s/P_b = 200$; and d) $P_s/P_b \to \infty$.**

Figure 7 shows the rotational temperature distribution along the $(x, 0, 0)$ axis. The experimental data for this variable are available only for $X/D < 8.0$, and the two cases $P_s/P_b = 220$ and $P_s/P_b \to \infty$ agree well with experimental data.

The effects of $L/D$ are further shown in Fig. 8, which shows the density distribution along the $(x, 0, 0)$ axis for $Kn_s = 0.002$, $P_s/P_b = 220$, at different values of $L/D$. It can be seen that increasing $L/D$ values leads to smaller peaks, or weaker interactions between the two jets. Although the Mach disk is weak and diffused in the secondary jet, it can be found that, for all $L/D$ values (except $L/D = 8.0$), the location of the Mach disk in the secondary jet does not differ significantly ($X_{M,\text{secondary}}/D \approx 13$). This may be due to the large $P_s/P_b$ value used ($P_s/P_b = 220$). When $X/D$ is large, based on the definition of $Kn_p(\theta)$ [Eq. (4)], the plumes from the two jets become much more rarefied and are fully mixed in the interaction region.

The effects of $Kn_s$ are shown in Fig. 9, which plots the density distribution along the $(x, 0, 0)$ symmetry axis for $P_s/P_b = 200$, $L/D = 3.0$, at different values of $Kn_s$. Reducing the $Kn_s$ values increases the interaction between the two jets (higher peaks). When $Kn_s$ is relatively large ($Kn_s = 0.02$), the flow is strongly rarefied and no Mach disk is formed in the interaction region.

The effects of $P_s/P_b$ ($Kn_s = 0.005$, $L/D = 3.0$) are shown in the density plot of Fig. 10. It can be observed that the peak values of density occur at approximately $X/D = 3$. Reducing $P_s/P_b$ strengthens the interaction between the secondary jet and the background gas. When $P_s/P_b$ is small, a stronger Mach disk is formed in the secondary jet and its location moves upstream. It can be seen that the existence of the background pressure significantly modifies the secondary jet flows, even when $X/D$ is small. This is not the case for the primary jets, where the background gas does not significantly affect the expansion core within the zone of silence when $Kn$ is small. The reason may be found in the small density values in the secondary jet, relative to the primary jets. Therefore, the molecules of the background gas can penetrate into the secondary jet flow more easily.

The thermal nonequilibrium effects in the interacting jets are also investigated. Because the secondary jet is more rarefied, significant deviation between the translational and rotational curves are observed. Figure 11 shows the translational and rotational temperature profiles along the $(x, 0, 0)$ symmetry axis for $Kn_s = 0.005$, $L/D = 3.0$, and different values of $P_s/P_b$. The background gas affects nonequilibrium in the secondary jet. Specifically, the figure shows that the smaller the values of $P_s/P_b$, the smaller the deviation between the two temperatures.

## IV. Conclusions

The simulations carried out in this Note are the first for interacting rarefied jets expanding into a background with finite pressure. The findings, such as the effects of the background gas on the shock structure, the rarefaction, and the thermal nonequilibrium effects in the secondary jet appear to be correct and can be explained from the physics of the problem.



## References


[1] Houshang, B. E., Levine, J., and Kawasaki, A., "Numerical Investigation of Twin-Nozzle Rocket Plume Phenomenology," *Journal of Propulsion and Power*, Vol. 16, No. 2, 2000, pp. 178–186. doi:10.2514/2.5572

[2] Dagum, L., and Zhu, S. H. K., "Direct Simulation Monte Carlo Simulation of the Interaction Between Rarefied Free Jets," *Journal of Spacecraft and Rockets*, Vol. 31, No. 6, 1994, pp. 960–964. doi:10.2514/3.26544

[3] Dankert, C., and Koppenwallner, G., "Experimental Study of Interaction between Two Rarefied Free Jets," *Rarefied Gas Dynamics: Proceeding of the 14th International Symposium on Rarefied Gas Dynamics*, edited by H. Oguchi, Univ. of Toyko Press, Tokyo, 1984, pp. 477–484.

[4] Ladeinde, F., Cai, X., Li, W., and Agarwal, R., "A Unified Computational Methodology for Rarefied and Continuum Flow Regimes," AIAA Paper 2004-1178.

[5] Wu, J.-S., Chou, S.-Y., Lee, U.-M., Shao, Y.-L., and Lian, Y.-Y., "Parallel DSMC Simulation of a Single Under-Expanded Free Orifice Jet from Transition to Near-Continuum Regime," *Journal of Fluids Engineering*, Vol. 127, 2005, pp. 1161–1170. doi:10.1115/1.2062807

[6] Bird, G. A., *Molecular Gas Dynamics and the Direct Simulation of Gas Flows* 1st ed., Oxford Univ. Press, Oxford, England, U.K., 1994, pp. 1–484.

[7] Marrone, P. V., "Temperature and Density Measurements in Free Jets and Shock Waves," *Physics of Fluids*, Vol. 10, 1967, pp. 521–538. doi:10.1063/1.1762146

[8] Mori, H., Niimi, T., Akiyama, I., and Tsuzuki, T., "Experimental Detection of Rotational Non-Boltzmann Distribution in Supersonic Free Molecular Nitrogen Flows," *Physics of Fluids*, Vol. 17, 2005, Paper 117103. doi:10.1063/1.2130752

[9] Young, W. S., "Derivation of the Free-Jet Mach-Disk Location Using the Entropy-Balance Principle," *Physics of Fluids*, Vol. 18, No. 11, 1975, pp. 1421–1425. doi:10.1063/1.861039

[10] *AEROFLO's User Manual*, TTC Technologies, Centereach, NY, 2004.

[11] Li, W., "Analysis of Single and Dual Underexpanded Rarefied Jets," Ph.D. Dissertation, Dept. of Mechanical Engineering, Stony Brook Univ., Stony Brook, NY, 2010, pp. 62–68.

[12] Muntz, E. P., Hamel, B. B., and Maguire, B. L., "Some Characteristics of Exhaust Plume Rarefaction," *AIAA Journal*, Vol. 8, No. 9, 1970, pp. 1651–1658. doi:10.2514/3.49856

[13] Ashkenas, H., and Sherman, F. S., "The Structure and Utilization of Supersonic Free Jets in Low Density Wind Tunnels," *Rarefied Gas Dynamics, Fourth Symposium*, Vol. 2, Academic Press, New York, 1966, pp. 311–330.

[14] Crist, S., Sherman, F. S., and Glass, D. R., "Study of Highly Under-Expanded Sonic Jet," *AIAA Journal*, Vol. 4, 1966, pp. 68–71. doi:10.2514/3.3386

[15] Soga, T., Takanishi, M., and Yasuhara, M., "Experimental Study of Interaction of Underexpanded Free Jets," *Rarefied Gas Dynamics: Proceedings of the 14th International Symposium on Rarefied Gas Dynamics*, Tsukuba Science City, Japan, edited by H. Oguchi, Univ. of Toyko Press, Tokyo, July 1984, pp. 485–493.


S. Fu
*Associate Editor*